



Loss-of-Function Plays a Major Role in Early Neurogenesis of Tubulin α -1 A (*TUBA1A*) Mutation-Related Brain Malformations

Liangqun Xie¹ · Jingrui Huang¹ · Lei Dai¹ · Jiefeng Luo¹ · Jiejie Zhang¹ · Qiaozhen Peng¹ · Jingchi Sun¹ · Weishe Zhang^{1,2} 

Received: 26 February 2020 / Accepted: 30 October 2020
© Springer Science+Business Media, LLC, part of Springer Nature 2020

Abstract

Tubulin α -1 A (*TUBA1A*) mutations cause a wide spectrum of brain abnormalities. Although many mutations have been identified and functionally verified, there are clearly many more, and the relationship between *TUBA1A* mutations and brain malformations remains unclear. The aim of this study was to identify a *TUBA1A* mutation in a fetus with severe brain abnormalities, verify it functionally, and determine the mechanism of the mutation-related pathogenesis. A de novo missense mutation of the *TUBA1A* gene, c.167C>G p.T56R/P.THR56Arg, was identified by exon sequencing. Computer simulations showed that the mutation results in a disruption of lateral interactions between the microtubules. Transfection of 293T cells with *TUBA1A* p.T56R showed that the mutated protein is only partially incorporated into the microtubule network, resulting in a decrease in the rate of microtubule re-integration in comparison with the wild-type protein. The mechanism of pathological changes induced by the mutant gene was determined by knockdown and overexpression. It was found that knockdown of *TUBA1A* reduced the generation of neural progenitor cells, while overexpression of wild-type or mutant *TUBA1A* promoted neurogenesis. Our identification and functional verification of the novel *TUBA1A* mutation extends the *TUBA1A* gene-phenotype database. Loss-of-function of *TUBA1A* was shown to play an important role in early neurogenesis of *TUBA1A* mutation-related brain malformations.

Keywords Loss-of-function · Whole-exome sequencing (WES) · *TUBA1A* · Neurogenesis · Brain malformation

Introduction

Since the discovery in 2007 that the *TUBA1A* gene is implicated in brain malformation, at least 121 distinct *TUBA1A* mutations in a total of more than 166 patients have been identified [1, 2]. These pathogenic mutations are located throughout the sequence of the gene and result in a wide range of brain malformations [3]. The defects in brain development include lissencephaly, polymicrogyria-like cortical malformations, and a mildly simplified or unaffected cerebrocortical surface

[1, 4–8]. The analysis of the type and localization of all possible 2969 missense variants of the *TUBA1A* gene predicted that a large majority of *TUBA1A* missense variants are deleterious [2]. Therefore, the discovery of additional mutations and their clinical manifestations can be anticipated.

The clinical effects of mutations are always consistent with the role of the gene and the impact of the mutation site on its function. *TUBA1A* encodes the tubulin α -1 A chain, which is an important component of microtubules. Microtubules have an important role during mitosis and in the dendrites and axons of nerve cells. Since *TUBA1A* is highly expressed in the fetal brain [8, 9], mutations leading to microtubule dysfunction will undoubtedly result in brain malformation. Identified *TUBA1A* mutations in the clinic have underscored the possibility that *TUBA1A* mutations cause microtubule defects. Protein modeling of the identified sites of mutations and cell functional studies suggested that some mutations result in defective interactions in the tubulin heterodimer assembly pathway, while others may alter the three-dimensional conformation of the *TUBA1A* protein and/or compromise its interaction with microtubule-associated proteins (MAPs) or

Supplementary Information The online version contains supplementary material available at <https://doi.org/10.1007/s12035-020-02193-w>.

✉ Weishe Zhang
zhangweishe@yeah.net

¹ Department of Obstetrics, Xiangya Hospital Central South University, 87 Xiangya Road, Changsha 410008, China

² Hunan Engineering Research Center of Early Life Development and Disease Prevention, 87 Xiangya Road, Changsha 410008, China

microtubule motors such as kinesin [10]. However, because *TUBA1A* mutations are not clustered in any specific region of the gene, the identification of mechanisms responsible for brain malformations remains challenging.

Based on clinical information and functional studies, two conflicting hypotheses explaining the mechanism of the impact of *TUBA1A* mutations have been advanced: a dominant-negative effect and a loss-of-function mechanism. The evidence supporting the dominant-negative effect is as follows: (1) all *TUBA1A* mutations identified thus far are missense rather than frameshift or truncation mutations; (2) modeling of *TUBA1A* mutations in yeast revealed that numerous α -tubulin disease-associated mutants do not behave as null alleles; and (3) some *TUBA1A* mutations do not affect the ability of the α -tubulin protein to integrate into the endogenous microtubule network [11–13]. On the other hand, the loss-of-function hypothesis is supported by the following: (1) several large cytogenetics databases and the results of screening 15,000 subjects with developmental disorders do not provide any indication of the deletion mutation in *TUBA1A*, indicating that this type of mutation may cause early embryonic death; (2) cell functional studies have shown that certain mutations result in defects in the interactions in the tubulin heterodimer assembly pathway; and (3) some mutations result in a moderate to severe decrease in the incorporation of α -tubulin into microtubules [14, 15]. However, whether these two hypotheses apply to neurodevelopmental processes has not been studied.

The present investigation identified a new mutation site in the *TUBA1A* gene. Protein simulation and functional verification of this mutation site were performed using 293T cells. Two hypotheses concerning the mechanism by which a single-point mutation of *TUBA1A* can cause severe brain deformities were presented. To determine the role of these two mechanisms in neural development, human embryonic stem (hESC) knockdown and overexpression models were generated.

Materials and Methods

Clinical Report

The present study originated from a routine clinical diagnostic work-up. The fetus was the second pregnancy of a healthy Chinese non-consanguineous couple (a 34-year-old mother and a 35-year-old father) and was conceived using IVF-ET. The first pregnancy of this couple resulted in miscarriage. The fetus appeared normal at an early examination, but at 18 weeks of gestation (GW), ultrasonography revealed a slightly smaller head, biparietal diameter of 38 mm, and small size of the cerebellum. Amniocentesis was performed for prenatal diagnostics and shown a normal karyotype of the fetus.

Gene microarray indicated no abnormal copy number variants. At 25 + 1 GW, ultrasonography documented cerebellar dysplasia with hydrocephalus and the absence or dysplasia of the hyaline septum; corpus callosum dysplasia was not excluded. The head is small (Supplementary Fig. 1). After obtaining written informed consent from the parents, the pregnancy was terminated at 26 + 5 GW. The post-mortem examination of the fetus demonstrates female sex, hydrocephalus, atrophy of brain tissue, decrease in neurons, loss of corpus callosum, and cerebellar atrophy (Supplementary Fig. 2).

Whole-Exome Sequencing (WES)

Exome sequencing was performed by the BGI Genomics (Wuhan, China). The parents' consent was obtained using a standard consent form provided by the BGI. Briefly, genomic DNA was extracted from fetal skin; DNA exons were captured utilizing a SureSelect platform (Agilent Technologies, Santa Clara, CA, USA); then, libraries were prepared, and they were sequenced by a HiSeq2500 Analyzer (Illumina, San Diego, CA, USA) according to the manufacturer's instructions for paired-end 200–250 bp reads. Sequencing reads were aligned against the human genome reference sequence (GRCh37/hg19). Variants were annotated using public databases (dbSNP137, gnomAD, ExAC, the 1000 Genomes Project, ESP6500) and the HGMD Professional database. Variant pathogenicity was predicted by the SIFT and PolyPhen-2 software. Possible pathogenic variants were validated by Sanger sequencing.

Structural Modeling of *TUBA1A* Mutations

The missing residues 35–60 in α -tubulin of the tubulin dimer structure (PDB code: 1JFF, resolution: 3.5 Å) were modeled by homology modeling using the SWISS-MODEL server (<https://swissmodel.expasy.org/>). Subsequently, the entire structures were docked into the density map (MT-13-3, EMDB code: EMD-5193) using UCSF Chimera [16, 17] to construct polymerized microtubule structures. The three-dimensional structure of the protein with the p.T56R mutation was analyzed in UCSF Chimera with restrained local energy minimization. Finally, PyMOL [18] was employed to analyze lateral interactions and to generate images.

Cell Culture

Two hundred ninety-three T cells (no. SCSP-502) were purchased from the Cell Bank of the Chinese Academy of Science (Shanghai, China) and cultured in DMEM (Gibco, USA) supplemented with 10% FBS (Gibco, USA) media at 37 °C and 5% CO₂. The H9 line of human embryonic stem cells (hESC 9) was cultured as previously described [19].

Microtubule Incorporation and Polymerization Tests

The full-length wild-type and mutant *TUBA1A* cDNA sequences were synthesized by Plectrum Biology Co., Ltd. (Changsha, China). The cDNA sequences were cloned into a p3XFLAG-CMV-14 plasmid (Sigma, St Louis, MO, USA) to generate two independent C-terminally FLAG-tagged *TUBA1A* wild-type (CMV-TUBA1A(WT)-3xFlag) and mutant (CMV-TUBA1A(MU)-3xFlag) plasmids. Subsequently, the plasmids were transfected into 293T cells grown on glass coverslips using Lipofectamine3000 (Invitrogen, USA). To determine the incorporation of tubulin α -1 A into microtubules, after 24 h, the cells were stained using fluorescent-labeled antibodies against the FLAG antibody to detect the expression of the transgene and against α -tubulin to detect the endogenous microtubule network. In the microtubule re-polymerization assay, transfected 293T cells were incubated at 4 °C for 30 min and then returned to 37 °C. Immunolabeling for FLAG and α -tubulin was performed immediately after transferring to 37 °C and 15 and 30 min later.

Establishment of *TUBA1A* Knockdown and Overexpression hESCs

For the establishment of knockdown hESCs, two short hairpin RNA (shRNA) sequences (Supplementary Table 1) are cloned into the CD511B-U6-lentivector (with a GFP marker) to form CD511B-U6-shRNA1&2 lentiviral plasmids. Then, lentivirus packaging was performed: 6 μ g of the lentiviral vector (CD511-U6, CD511B-U6-shRNA1&2) and 4 μ g of PMDL, 3 μ g of VSV-G, and 2 μ g of Rev were co-transfected into 293T cells using Lipofectamine3000, at 24–72 h after transfection; the supernatant containing viral particles was collected and concentrated. For hESC9 infection, the cells were detached from the surface using Accutase (STEMCELL Technologies, Canada), resuspended to form a single-cell suspension and re-seeded in Matrigel-coated 6-well plates. After 24 h, 10 μ l of the virus suspension was added to each well, and the medium was replaced with fresh PSCeasy® hESC/hiPSC medium (Cellapy, China) after 12 h. Cells were selected by flow cytometry (FCM) 48 h after the transfection.

For the establishment of hESCs overexpressing *TUBA1A*, full-length wild-type and mutant *TUBA1A* cDNA sequences were cloned into the lentiviral GTP-CMV-vector with a GFP marker. This protocol was performed by the Biolink Biotechnology Co., Ltd. (Changsha, China). The lentivirus packaging protocol was the same as knockdown groups, with the only difference that the transfected cells were selected by 2 μ g/ml puromycin (Sigma) for 2 weeks.

Neural Progenitor Cells (NPCs) and Neuronal Differentiation

hESCs were differentiated into NPCs according to a previously published protocol [20]. Briefly, the hESC9 cells were dissociated into single cells and incubated in E6 medium (Gibco, USA) supplemented with dual SMAD inhibitors, LDN193189 (0.1 mM) and SB431542 (10 mM), for 7 days.

hESCs were differentiated into neurons according to the protocol provided by the STEMdiff™ neuron differentiation kit (STEMCELL Technologies). Briefly, the cells were allowed to form embryoid bodies using AggreWell 800 plates (STEMCELL Technologies) for 5 days in STEMdiff™ neural induction medium (STEMCELL Technologies). The embryoid bodies were re-seeded onto poly-L-ornithine/laminin (Sigma)-coated plates to obtain attachment cultures and maintained in STEMdiff™ neural induction medium for an additional 6 days. Then, the cells were dissociated with Accutase, and the above medium was replaced with STEMdiff™ neuronal differentiation medium for further culture.

Immunofluorescence Staining

Immunofluorescence staining was performed as previously described [21, 22]. Cell images were acquired using a fluorescence microscope (Nikon, Japan or Zeiss LSM 880 with Airyscan, Germany). The primary and secondary antibodies used are listed in Supplementary Table 2.

Western Blotting

Western blotting was conducted as previously described [23, 24]. The primary and secondary antibodies used are listed in Supplementary Table 2.

Real-Time Quantitative PCR (qRT-PCR) Analysis

qRT-PCR was performed as previously described [19, 25]. The primer sequences are listed in Supplementary Table 3.

Image Analysis

To understand the effect of the *TUBA1A* p.T56R mutation on the incorporation and re-polymerization of microtubules in vitro, we used the ImageJ software (NIH, Bethesda, MD, USA) with the Coloc 2 plug-in to measure the Manders' colocalization coefficients (M1) of FLAG and endogenous α -tubulin, according to previously published protocols [26, 27]. The M1 coefficient is defined as: $M1 = \sum R_i \cdot \text{colocal} / \sum R_i$. Values for this coefficient range from 0 to 1 and express the sum of the intensities of red pixels that have a green component divided by the total red intensity values, that is, the percentage of colocalization of TUBA1A WT or

p.T56R and the endogenous α -tubulin cytoskeleton. Results were transferred to GraphPad Prism 6.0 (GraphPad Software, San Diego, CA, USA) for statistical analysis.

Statistical Analysis

All data are presented as the mean \pm SEM. Data were analyzed using GraphPad Prism, version 6.0 (GraphPad Software). The Student's *t* test was applied to compare the differences between groups. $P < 0.05$ was considered statistically significant.

Results

Identification of *TUBA1A* p.T56R as the Pathogenic Variant by Exome Sequencing

Exome sequencing identifies three candidate causative variants (Table 1). The detected mutation *TUBA1A* p.T56R (p.THR56Arg c.167 C>G) is not listed in public databases; however, according to the HGMD database, this mutation affects amino acid residues already found to be involved in a different substitution (CM145639, p.T56M) which is highly conserved in many species (Fig. 1a). The SIFT and PolyPhen-2 scores indicated the harmfulness of the substitution based on the reports that the *TUBA1A* missense mutation can result in brain malformation. On this basis, the *TUBA1A* p.T56R mutation was considered to represent a pathogenic variant. Among the other two missense mutations, WDR62 p.(=) (alt:p.G248G C.744C > A) is a synonymous mutation and is scored as harmless by SIFT and PolyPhen-2. According to previous reports, the PCNT p.k3134T (p.lys3134thr c.9401A>C) mutation is a homozygous mutation or complex heterozygous mutation causing brain abnormalities. Sanger sequencing confirmed that the WDR62 p.(=) mutation detected in the fetus was inherited from the father, and PCNT p.k3134T was inherited from the mother. Importantly, the *TUBA1A* p.T56R mutation is not detected in the parents (Fig. 1b, c). Thus, in accordance with the guidelines of the American College of Medical Genetics and Genomics (ACMG), *TUBA1A* p.T56R was judged as the causative genetic variation in this fetus.

TUBA1A p.T56R Alters the Structural Stability of the Lateral Interactions Between Microtubules

The identified *TUBA1A* p.T56R mutation is located in the H1'-S2 ring region at the N-terminal of α -tubulin and is predicted to be associated with lateral interactions between microtubules (Fig. 2a-c). The side chain of Thr56 is a short structure, and it forms a hydrogen bond with Gln128 of its own chain, increasing its proximity to the His283 of another α -tubulin molecule (Fig. 2d). However, the T56R mutation results in an increase in the length of the side chain, which can simultaneously form hydrogen bonds with Gln128 of its own chain and His283 of another α -tubulin molecule (Fig. 2e). Therefore, due to the increase in the number of hydrogen bonds, the T56R mutation is expected to lead directly to closer lateral interactions between the α -tubulin molecules.

Effect of the *TUBA1A* p.T56R Mutation on the Incorporation into Microtubules and Re-polymerization in vitro

To further investigate the in vitro functional consequences of the *TUBA1A* p.T56R mutation, wild-type and p.T56R constructs were transiently expressed in 293T cells. In the microtubule incorporation assays, *TUBA1A* p.T56R was integrated into microtubules at a lower level than that of the wild-type protein (Fig. 3a, b). During microtubule re-polymerization, at 15 and 30 min, p.T56R demonstrated at 15 and 30 min a remarkable persistence of the more diffuse high background of the label than that observed for the wild-type α -tubulin, reflecting a reduced rate of microtubule re-integration for the mutant form of this protein (Fig. 3c, d). These results indicate that the p.T56R mutation affected microtubule incorporation and re-polymerization.

Mechanism of Brain Malformation Caused by *TUBA1A* Mutations

The demonstrated effects of *TUBA1A* mutations emphasize the gene's importance in brain development. However, because mutations are widely distributed throughout the *TUBA1A* gene, two conflicting hypotheses regarding the underlying mechanism have been raised: loss-of-function and

Table 1 Detailed information on the three candidate causative variants identified in the fetus

Gene	Reference sequence	Variant	Exon	Heterozygosity	Chromosome	Variation type
<i>TUBA1A</i>	NM-001270399.1	c.167C>G, p.T56R/P.THR56Arg	ex2	het	Chr12:49580453	VUS ^a
PCNT	NM-006031.5	c.9401A>C, p.k3134T p.lys3134thr	ex43	het	Chr21:47860775	VUS ^a
WDR62	NM-001083961.1	c.744C>A, p.(=)(alt:p.G248G)	ex7	het	Chr19:36558774	VUS ^a

^a Variant of undetermined significance

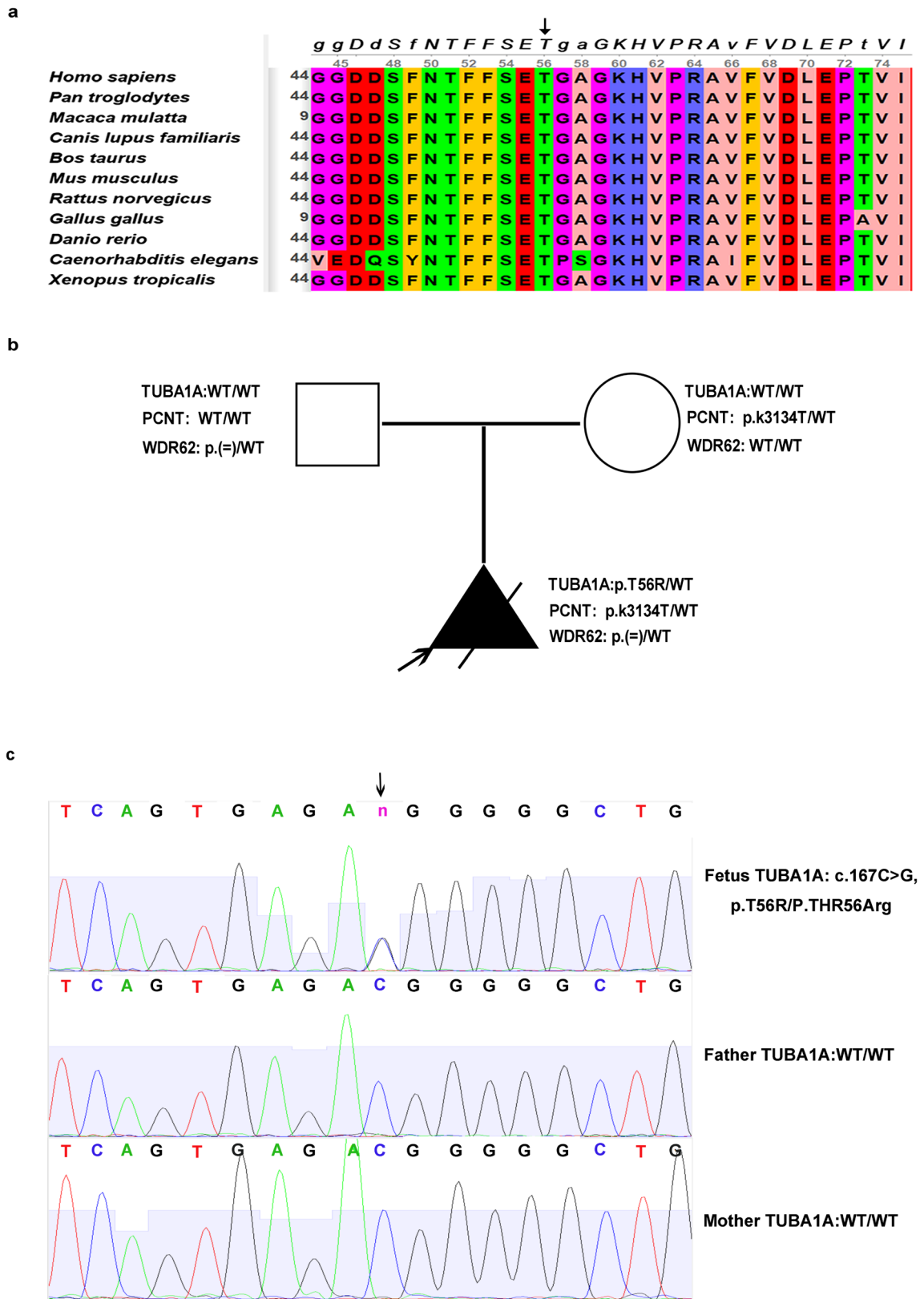


Fig. 1 Identification of TUBA1A p.T56R in a fetus with a brain malformation. **a** The affected amino acid is conserved in many species. **b** Pedigree analysis; the fetus is represented by a filled symbol. WT, wild-type. **c** Genomic DNA sequence chromatograms indicating the position of the c. 167 C>G mutation

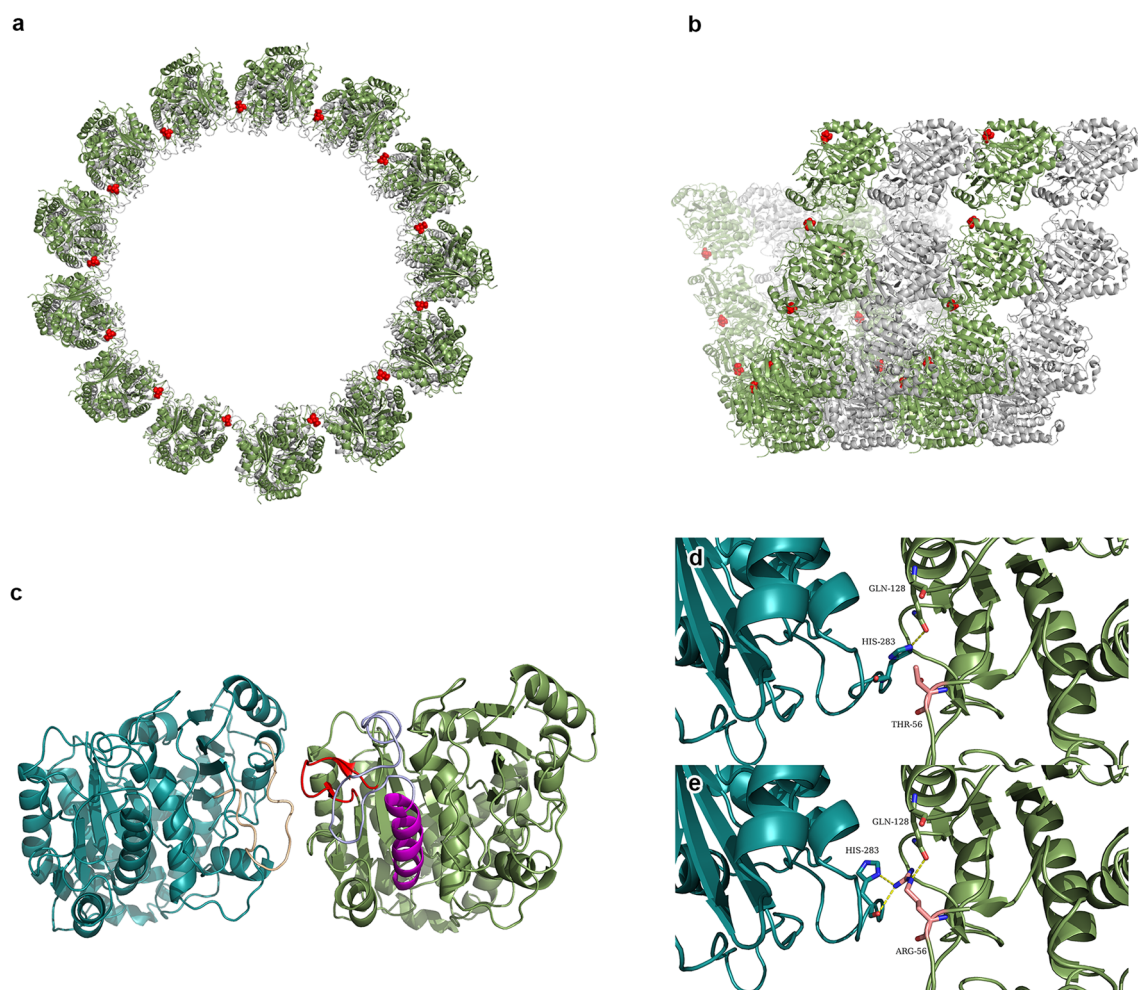


Fig. 2 Three-dimensional modeling of TUBA1A p.T56R in a microtubule structure. **a** Top view of a microtubule illustrating 13 longitudinal protofilaments forming a microtubule via lateral interactions. Green represents α -tubulin, gray represents β -tubulin, and red represents the T56 residue. **b** Side view of a microtubule. **c** Higher resolution image of the lateral interaction between two α -tubulin

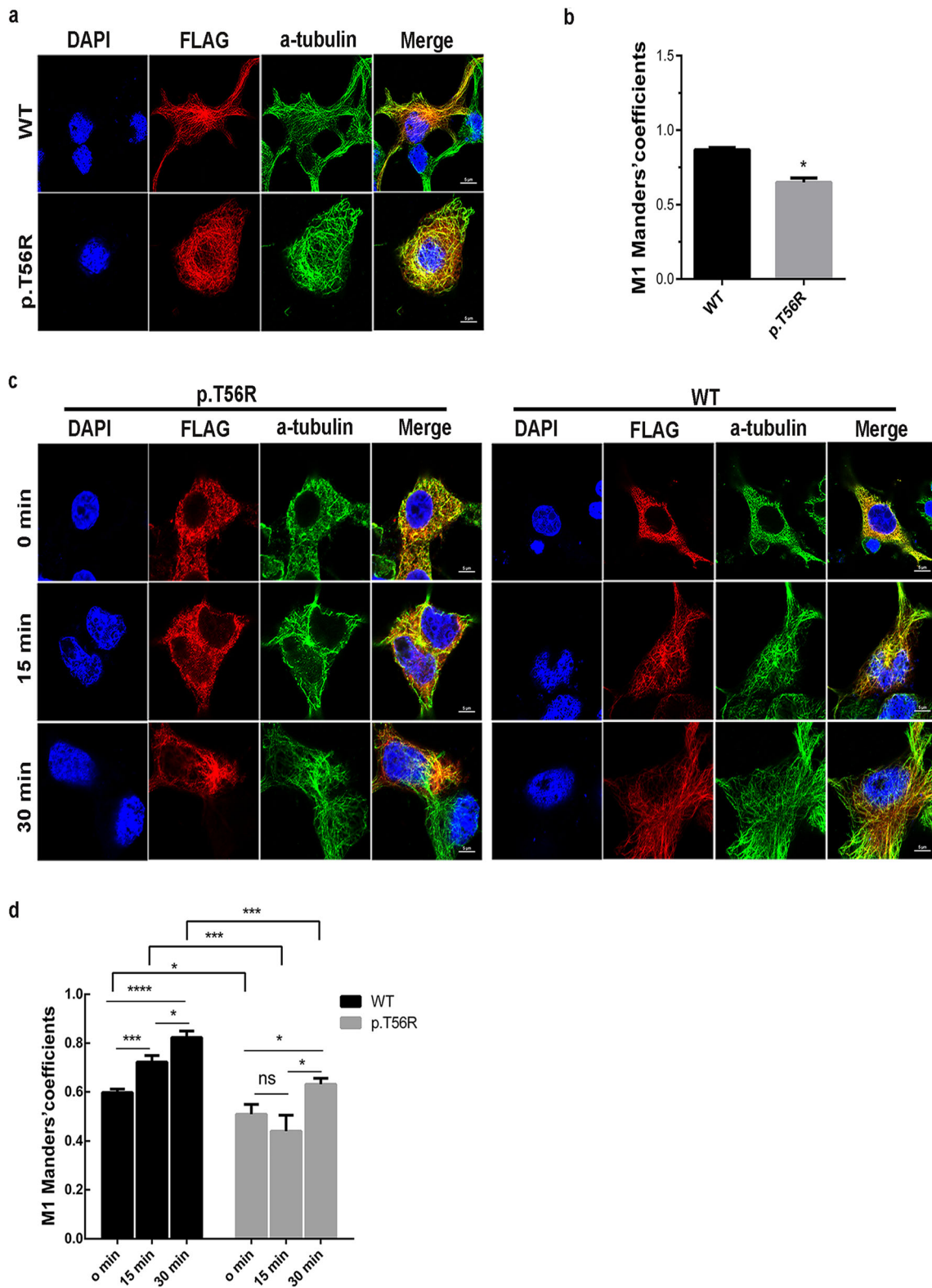
molecules (green and dark blue). Gold represents the M loop, red represents the H1'-S2 loop, and magenta represents the H1 helix. The T56 residue is located in the H1'-S2 loop region. **d** The T56 residue forms hydrogen bonds with Gln128 in the same monomer, allowing His283 of another alpha-tubulin molecule to be in close proximity. **e** The R56 residue forms a hydrogen bond with both His283 and Gln128

dominant-negative effects. Subsequent experiments were designed to test these two possibilities.

To investigate the impact of *TUBA1A* loss-of-function in neurodevelopment, two specific *TUBA1A* knockdown lentivirus plasmids (CD511B-U6-shRNA1&2) were transduced into hESCs, using CD511-U6 empty vector-transduced hESCs as a control. GFP-positive transduced hESCs are selected by FCM (Supplementary Fig. 3a) to form stable cell lines, and western blot confirms that the shRNA1 and shRNA2 cell lines reduced *TUBA1A* protein by approximately 50% compared to control cells (Fig. 4a). The two cell lines had a normal karyotype and displayed pluripotency and trilineage differentiation potential, but their proliferation ability is slightly decreased (Supplementary Fig. 3b–f). Next, the cell lines were stimulated to differentiate into neural progenitor cells (NPCs). *TUBA1A* knockdown cell lines, the expression of NPC marker PAX6 was significantly reduced at day 7 (Fig. 4b, c). To

confirm this result, we also explore the expression of *TUBA1A* in non-transfected hESCs differentiated into NPCs; the expression of *TUBA1A* gradually increases during the differentiation of hESCs into NPCs (Supplementary Fig. 3g), a

Fig. 3 Effect of *TUBA1A* p.T56R on microtubule incorporation and repolymerization in vitro. **a** In comparison with the wild-type protein, much of the *TUBA1A* p.T56R mutated protein cannot colocalize with the α -tubulin cytoskeleton, indicating a reduction of *TUBA1A* p.T56R incorporation into microtubules. Scale bar = 5 μ m. **b** Quantitative analysis of the percentage of *TUBA1A* WT or p.T56R colocalized with the endogenous α -tubulin cytoskeleton. *TUBA1A* WT, $n = 27$ *TUBA1A* p.T56R, $n = 26$, $*P < 0.05$. **c** After 15 and 30 min at 37 $^{\circ}$ C, the wild-type α -tubulin is re-incorporated into microtubules, while *TUBA1A* p.T56R continues to be diffusely distributed in the cytoplasm. Scale bar = 5 μ m. **d** Quantitative analysis of the percentage of colocalization of *TUBA1A* WT or p.T56R and the endogenous α -tubulin cytoskeleton after 0 s, 15 min, and 30 min of rewarming. 0 s, 15 min, 30 min *TUBA1A* WT, $n = 25$ –30 *TUBA1A* p.T56R, $n = 25$ –30. $*P < 0.05$, $**P < 0.01$, $***P < 0.001$, and $****P < 0.0001$



result consistent with previous studies on iPS-NPCs [28]. These results indicate that a normal dose of *TUBA1A* protein is essential at the NPC stage of hESC differentiation.

To investigate the dominant-negative hypothesis, hESCs were transduced with lentivirus expressing a wild-type protein, *TUBA1A* with the p.T56R mutation, or *TUBA1A* with the

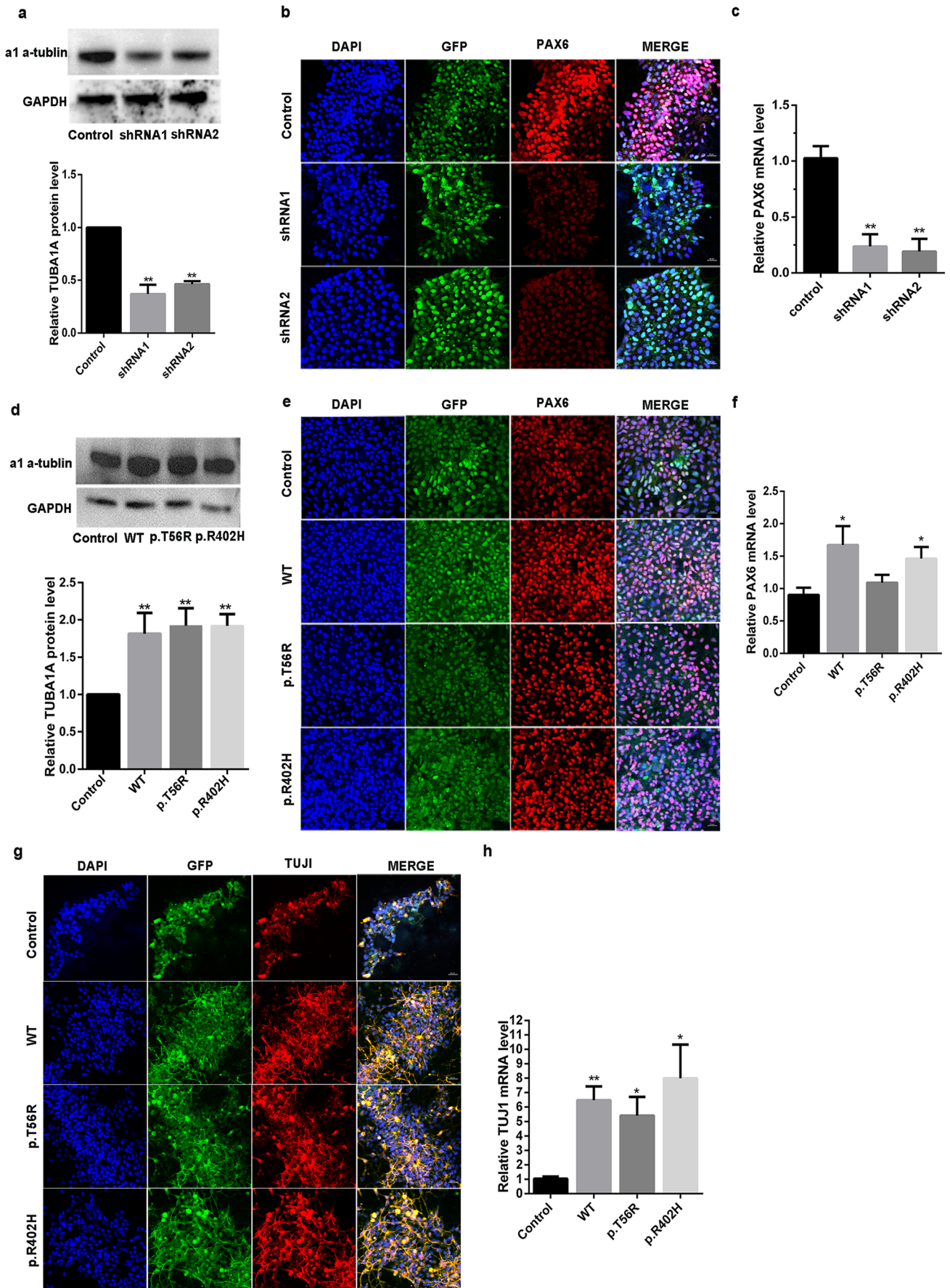


Fig. 4 The effect of *TUBA1A* loss-of-function on neural differentiation of hESC. **a** Western blot analysis of *TUBA1A* expression in control, shRNA1, and shRNA2 hESCs. Results are shown relative to control ($n = 3$). **b** Immunostaining of the neural progenitor marker PAX6 in control, shRNA1, and shRNA2 hESCs 7 days after the induction of neural differentiation. Scale bar = 20 μm . **c** qRT-PCR analysis of PAX6 expression in control, shRNA1, and shRNA2 hESCs 7 days after the induction of neural differentiation ($n = 5-6$). **d** Western blot analysis of *TUBA1A* expression in control, wild-type, p.T56R, and R402H hESCs. Results are shown relative to control ($n = 4$). **e** Immunostaining of PAX6 in control, wild-type, p.T56R, and R402H hESCs 7 days after the induction of neural differentiation. Scale bar = 20 μm . **f** qRT-PCR analysis of PAX6 expression in control, wild-type, p.T56R, and R402H hESCs 7 days after the induction of neural differentiation ($n = 4-6$). **g** Immunostaining of the neuronal marker TUJ1 in control, wild-type, p.T56R, and R402H hESCs 15 days after the induction of neural differentiation. Scale bar = 20 μm . **h** qRT-PCR analysis of the TUJ1 expression in control, wild-type, p.T56R, and R402H hESCs 15 days after the induction of neural differentiation ($n = 3$)

p.R402H mutation, using GTP-CMV-empty vector-transduced hESCs as a control. The p.R402H substitution is a frequently reported recurrent *TUBA1A* mutation. After puromycin selection, hESCs are GFP-positive (Supplementary Fig. 4a), indicating successful transduction with the constructs. Western blot analysis revealed that, in comparison with control cells, the alpha-tubulin protein levels of are increased 1.8–1.9-fold in wild-type, p.T56R, and p.R402H-expressing cell lines (Fig. 4d). Forced expression of *TUBA1A* is not sufficient to drive neural differentiation of hESCs, which retained normal karyotypes, pluripotency, and trilineage differentiation potential (Supplementary Fig. 4b–e). Upon differentiation into NPCs, cells overexpressing wild-type and p.R402H had significantly increased expression of PAX6 at day 7, while overexpression of p.T56R also shows a trend towards upregulation of this protein (Fig. 4e, f). The differentiation into neurons, measured by the neuronal marker TUJ1 at day 15, is more efficient in cells expressing wild-type *TUBA1A* and *TUBA1A* with p.R402H or p.T56R mutations than in the control cells (Fig. 4g, h). These data indicate that the mutant protein retains some of its normal functions and does not interfere with the activity of normal endogenous α -tubulin in the early stages of neural differentiation.

Discussion

The present investigation identified a novel de novo heterozygous missense mutation, *TUBA1A* p.T56R, in a fetus with severe brain malformations. In addition to *TUBA1A* p.C25F and p.R64W [29], p.T56R represents another *TUBA1A* mutation producing hydranencephaly-like dysplasias and expands the *TUBA1A* gene-phenotype database.

Protein modeling indicates that *TUBA1A* p.T56R is located in the H1'-S2 loop of α -tubulin and, therefore, can affect lateral interaction between microtubules. The above-mentioned

p.C25F and p.R64W mutations, as well as the earlier described p.T56M [30], p.E27Q [31], p.Y210C [32], p.D218Y [14], and p.G366R [33], are all located at sites affecting the lateral interaction of the microtubules, and all result in severe brain malformations. Therefore, it has been suggested that mutations in *TUBA1A* at positions essential for lateral interactions may lead to severe of brain malformations [29].

It has been previously proposed that the severity of nervous system damage may depend on the relative abundance of mutant α - and β -tubulin heterodimers compared with wild-type, combined with their ability to incorporate into the microtubule cytoskeleton, which may affect dynamics, motor protein, and MAP interactions in different dominant-negative ways [29, 34]. For example, p.R402H causes severe classic lissencephaly with complete agyria, while not influencing heterodimer formation and microtubule incorporation significantly [12, 14]. Similar properties are displayed by the mutants p.L286F [14] and p.P263T [12]. However, other findings suggest that some mutations, e.g., p.L397P [12], p.C25F, and p.R64W, which produce severe phenotypes, demonstrate a moderate to a severe decrease in incorporation into microtubules, adding an important caveat to this proposal. The current results demonstrated that the incorporation of p.T56R into the microtubule network is decreased. Therefore, the present findings are in agreement with the conclusion of Dr. Tischfield [34], who stated that there are not always clear phenotypic differences between the tubulin mutations that significantly diminish heterodimer formation and incorporation into microtubules and those that do not affect these properties. To understand the phenotype of the *TUBA1A* mutation, it is necessary to recognize first whether the pathogenic mechanism is due to a loss-of-function or is a dominant-negative effect.

To test the loss-of-function hypothesis, *TUBA1A* knock-down hESC lines were constructed. The original intent to knockout *TUBA1A* with CRISPR-Cas9, prompted by the possibility that constitutive knockout of *TUBA1A* might negatively affect the survival of hESCs, was not successful since none of the eight prepared guide RNAs yielded a positive clone (data not shown). After knocking-down *TUBA1A*, the hESCs formed significantly less PAX6-positive cells; and in hESC-NPCs and iPS-NPCs [28], the expression of *TUBA1A* was significantly increased. Based on these results, we propose that a normal dose of *TUBA1A* protein is essential for the formation of NPCs. Several other studies support this notion. For example, NPCs are located in the ventricular area and are the basis for the formation of the central nervous system (CNS). *TUBA1A* knockout can cause ventricular enlargement in mice due to disruption of NPC division [35], while *TUBA1A* knock-down can inhibit the formation of the zebrafish CNS [36]. In addition, the reported mutations of *TUBA1A* all resulted in ventricular dilatation [2, 37]; thus, it is reasonable to believe that mutations lead to a reduction in the normal

TUBA1A protein dose and thus reduce the generation of neural progenitor cells.

To test the dominant-negative effect hypothesis, wild-type, p.T56R, and p.R402H overexpressing hESC lines were constructed. A dominant-negative effect occurs when the proteins derived from the abnormal mutant allele interact with proteins from normal alleles, negatively interfering with their function. Thus, the introduction of a dominant-negative mutant of *TUBA1A* will interfere with the endogenous protein, leading to defects in neural differentiation. However, ectopic expression of the wild-type α -tubulin and the R402H mutant promoted NPC differentiation, significantly increasing the expression of PAX6 in the cells, while ectopic expression of p.T56R also upregulated PAX6, although to a lesser extent. Additionally, p.T56R promoted neuronal differentiation. These results indicate that the mutant protein does not affect the function of normal endogenous *TUBA1A* protein. Indeed, our research and the yeast *TUBA1A* mutant disease simulation system have shown that the mutant TUBA1A protein retains at least partially normal function that may vary depending on the mutation site, and these mutations do not result in any cytotoxic dominant-negative effects. For example, in the yeast *TUBA1A* mutant disease simulation system, yeast that has lost one copy of α -tubulin (single copy) will grow slowly, while any mutant plasmids, including those encoding TUBA1A N102D, N101S, R264C, R402C, R402H, and R422H, can rescue this phenotype, enhancing yeast growth rather than compromising the single normal copy of this protein and impairing growth. Even single-copy TUBA1A N101S, R264C, R402C, R402H, and R422H mutant yeast can maintain cell viability much like yeast bearing a single-copy WT version of this gene [13, 38]. Together, these findings and the results obtained in hESC with *TUBA1A* knockdown indicated that loss-of-function plays a major causative role in the *TUBA1A* mutation-induced abnormalities during early neurogenesis of the brain.

Some limitations of the present study should be acknowledged. Firstly, due to the sequence similarity between *TUBA1A* exon 2 and some regions of *TUBA1B* and *TUBA1C*, it is challenging and costly to generate patient hESCs bearing the p.T56R mutation or other mutations within the H1'-S2 ring through genome editing, preventing us from generating more conclusive proof that the loss of TUBA1A protein functionality is the mechanism whereby p.T56R or other mutations in the H1'-S2 loop that cause brain malformations. However, we can conclude that in the context of neural differentiation, p.T56R mutant TUBA1A exhibits partially normal functionality that does not interfere with the function of the normal endogenous TUBA1A protein, consistent with the conclusions of studies using a yeast TUBA1A mutant disease model system. When conducting experiments with a neurogenesis simulation using TUBA1A E27Q iPS cells, Shimojimathe et al. found that the neural differentiation

of patient-derived TUBA1A E27Q iPS cells did not differ significantly from that of control cells [39], indicating that E27Q does not impact neural differentiation via a dominant-negative effect. E27Q is located in the H1-H1' loop supporting the H1'-S2 loop and influences the lateral action of microtubules [40]. These findings may thus offer us some incidental insights into the mechanistic basis for the observed phenotypes. However, further stem cell-based knock-in experiments will be essential in the future in order to confirm and expand upon these findings. Therefore, we intend to screen the *TUBA1A* gene mutation sites in clinical patients with brain malformations, to obtain mutation-specific iPS cells to provide further direct evidence. Secondly, the development of the nervous system is complex and includes neuronal migration, and formation of synaptic connections, all affected by an internal and external environment. However, the present study has confirmed that *TUBA1A* loss-of-function plays an important role in early neurogenesis. Future studies will include three-dimensional neural simulation and in vivo transplantation.

In summary, the current investigation identified a novel de novo mutation of the *TUBA1A* gene, p.T56R. This mutation affects the lateral interaction of the microtubules, and, at least partially, the incorporation of α -tubulin into microtubules, reducing their rate of re-polymerization. The experiments utilizing hESCs with knockdown or overexpression of *TUBA1A* demonstrated that loss-of-function plays a major role in *TUBA1A* mutation-induced abnormalities of early neurogenesis in the brain.

Acknowledgments We are thankful to the affected fetus and their family members for their participation. We are grateful to Fang Chen from Kai Yuan's laboratory for using a laser confocal microscope (ZEISS LISM 880 with Airyscan) to help us take the immunofluorescence photos of microtubule incorporation and re-polymerization tests and neural differentiation.

Funding This research was funded by the National Natural Science Foundation of China (81974236, 81903696, 81571516), the Science and Technology Project of Hunan Province (2017SK2151, 2017SK1033), the National Key Research and Development Program of China (2016YFC1000206), and the National Twelfth-Five Year Research and Development Program of China (2014BAI05B05).

Availability of Data and Material The datasets generated during and/or analysed during the current study are available from the corresponding author on reasonable request.

Compliance with Ethical Standards

Conflict of Interest The authors declare that they have no conflict of interest.

Ethical Approval Experiments with human samples were approved by the medical ethics committee of the Xiangya Hospital of Centre South University. The procedures used in this study adhere to the tenets of the Declaration of Helsinki.

Consent to Participate The biological sample was obtained following written informed consent from its legal representatives.

Code Availability Not applicable

References

- Keays DA, Tian G, Poirier K, Huang GJ, Siebold C, Cleak J, Oliver PL, Fray M et al (2007) Mutations in alpha-tubulin cause abnormal neuronal migration in mice and lissencephaly in humans. *Cell* 128:45–57. <https://doi.org/10.1016/j.cell.2006.12.017>
- Hebebrand M, Hüffmeier U, Trollmann R, Hehr U, Uebe S, Ekici AB, Kraus C, Krumbiegel M et al (2019) The mutational and phenotypic spectrum of TUBA1A-associated tubulinopathy. *Orphanet J Rare Dis* 14(1):38. <https://doi.org/10.1186/s13023-019-1020-x>
- Bahi-Buisson N, Poirier K, Fourniol F, Saillour Y, Valence S, Lebrun N, Hully M, Bianco CF et al (2014) The wide spectrum of tubulinopathies: what are the key features for the diagnosis? *Brain* 137(6):1676–1700. <https://doi.org/10.1093/brain/awu082>
- Sohal AP, Montgomery T, Mitra D, Ramesh V (2012) TUBA1A mutation-associated lissencephaly: case report and review of the literature. *Pediatr Neurol* 46(2):127–131. <https://doi.org/10.1016/j.pediatrneurol.2011.11.017>
- Oegema R, Cushion TD, Phelps IG, Chung SK, Dempsey JC, Collins S, Mullins JG, Dudding T et al (2015) Recognizable cerebellar dysplasia associated with mutations in multiple tubulin genes. *Hum Mol Genet* 24(18):5313–5325. <https://doi.org/10.1093/hmg/ddv250>
- Romaniello R, Arrigoni F, Fry AE, Bassi MT, Rees MI, Borgatti R, Pilz DT, Cushion TD (2018) Tubulin genes and malformations of cortical development. *Eur J Med Genet* 61:744–754. <https://doi.org/10.1016/j.ejmg.2018.07.012>
- Gardner JF, Cushion TD, Niotakis G, Olson HE, Grant PE, Scott RH, Stoodley N, Cohen JS et al (2018) Clinical and functional characterization of the recurrent TUBA1A p.(Arg2His) mutation. *Brain Sci* 8(8). <https://doi.org/10.3390/brainsci8080145>
- Poirier K, Keays DA, Francis F, Saillour Y, Bahi N, Manouvrier S, Fallet-Bianco C, Pasquier L et al (2007) Large spectrum of lissencephaly and pachygyria phenotypes resulting from de novo missense mutations in tubulin alpha 1A (TUBA1A). *Hum Mutat* 28(11):1055–1064. <https://doi.org/10.1002/humu.20572>
- Myers KA, Bello-Espinosa LE, Kherani A, Wei XC, Innes AM (2015) TUBA1A mutation associated with eye abnormalities in addition to brain malformation. *Pediatr Neurol* 53(5):442–444. <https://doi.org/10.1016/j.pediatrneurol.2015.07.004>
- Friocourt G, Marcorelles P, Saugier-Verber P, Quille ML, Marret S, Laquerrière A (2011) Role of cytoskeletal abnormalities in the neuropathology and pathophysiology of type I lissencephaly. *Acta Neuropathol* 121(2):149–170. <https://doi.org/10.1007/s00401-010-0768-9>
- Tian G, Kong XP, Jaglin XH, Chelly J, Keays D, Cowan NJ (2008) A pachygyria-causing alpha-tubulin mutation results in inefficient cycling with CCT and a deficient interaction with TBCB. *Mol Biol Cell* 19(3):1152–1161. <https://doi.org/10.1091/mbc>
- Tian G, Jaglin XH, Keays DA, Francis F, Chelly J, Cowan NJ (2010) Disease-associated mutations in TUBA1A result in a spectrum of defects in the tubulin folding and heterodimer assembly pathway. *Hum Mol Genet* 19(18):3599–3613. <https://doi.org/10.1093/hmg/ddq276>
- Aiken J, Buscaglia G, Aiken AS, Moore JK, Bates EA (2019) Tubulin mutations in brain development disorders: why haploinsufficiency does not explain TUBA1A tubulinopathies. *Cytoskeleton (Hoboken)* 1(10):40–54. <https://doi.org/10.1002/cm.21567>
- Kumar RA, Pilz DT, Babatz TD, Cushion TD, Harvey K, Topf M, Yates L, Robb S et al (2010) TUBA1A mutations cause wide spectrum lissencephaly (smooth brain) and suggest that multiple neuronal migration pathways converge on alpha tubulins. *Hum Mol Genet* 19(14):2817–2827. <https://doi.org/10.1093/hmg/ddq182>
- Poirier K, Saillour Y, Fourniol F, Francis F, Souville I, Valence S, Desguerre I, Marie Lepage J et al (2013) Expanding the spectrum of TUBA1A-related cortical dysgenesis to polymicrogyria. *Eur J Hum Genet* 21(4):381–385. <https://doi.org/10.1038/ejhg>
- Pettersen EF, Goddard TD, Huang CC, Couch GS, Greenblatt DM, Meng EC, Ferrin TE (2004) UCSF Chimera—a visualization system for exploratory research and analysis. *J Comput Chem* 25(13):1605–1612. <https://doi.org/10.1002/jcc.20084>
- Huang CC, Meng EC, Morris JH, Pettersen EF, Ferrin TE (2014) Enhancing UCSF Chimera through web services. *Nucleic Acids Res* 42(Web Server issue):W478–84. <https://doi.org/10.1093/nar/gku377>
- Schrödinger, LLC. (2015) The PyMOL molecular graphics system, version 1.8, New York, NY: Schrödinger.
- Xie L, Huang J, Li X, Dai L, Lin X, Zhang J, Luo J, Zhang W (2019) Generation of a homozygous HDAC6 knockout human embryonic stem cell line by CRISPR/Cas9 editing. *Stem Cell Res* 41:101610. <https://doi.org/10.1016/j.scr.2019.101610>
- Chambers SM, Fasano CA, Papapetrou EP, Tomishima M, Sadelain M, Studer L (2009) Highly efficient neural conversion of human ES and iPS cells by dual inhibition of SMAD signaling. *Nat Biotechnol* 27(5):275–280. <https://doi.org/10.1038/nbt.1529>
- Xiao X, Yuan Q, Chen Y, Huang Z, Fang X, Zhang H, Peng L, Xiao P (2019) LncRNA ENST00000453774.1 contributes to oxidative stress defense dependent on autophagy mediation to reduce extracellular matrix and alleviate renal fibrosis. *J Cell Physiol* 234(6):9130–9143. <https://doi.org/10.1038/nbt.1529>
- Gu J, Wang Y, Cui Z, Li H, Li S, Yang X, Yan X, Ding C et al (2019) The construction of retinal pigment epithelium sheets with enhanced characteristics and cilium assembly using ips conditioned medium and small incision lenticule extraction derived lenticules. *Acta Biomater* 92:115–131. <https://doi.org/10.1016/j.actbio.2019.05.017>
- He L, Zhu W, Chen Q, Yuan Y, Wang Y, Wang J, Wu X (2019) Ovarian cancer cell-secreted exosomal miR-205 promotes metastasis by inducing angiogenesis. *Theranostics* 9(26):8206–8220. <https://doi.org/10.7150/thno.37455>
- Shen H, Yin L, Deng G, Guo C, Han Y, Li Y, Cai C, Fu Y et al (2018) Knockdown of Beclin-1 impairs epithelial-mesenchymal transition of colon cancer cells. *J Cell Biochem* 119(8):7022–7031. <https://doi.org/10.1002/jcb.26912>
- Duan RS, Liu PP, Xi F, Wang WH, Tang GB, Wang RY, Sajjilafu, & Liu CM. (2018) Wnt3 and Gata4 regulate axon regeneration in adult mouse DRG neurons. *Biochem Biophys Res Commun* 499(2):246–252. <https://doi.org/10.1016/j.bbrc.2018.03.138>
- Zinchuk V, Grossenbacher-Zinchuk O (2009) Recent advances in quantitative colocalization analysis: focus on neuroscience. *Prog Histochem Cytochem* 44(3):125–172. <https://doi.org/10.1016/j.proghi.2009.03.001>
- Cruzat A, Gonzalez-Andrades M, Mauris J, AbuSamra DB, Chidambaram P, Kenyon KR, Chodosh J, Dohlman CH et al (2018) Colocalization of Galectin-3 with CD147 is associated with increased gelatinolytic activity in ulcerating human corneas. *Invest Ophthalmol Vis Sci* 59(1):223–230. <https://doi.org/10.1167/iovs.17-23196>
- Bamba Y, Shofuda T, Kato M, Pooh RK, Tateishi Y, Takanashi J, Utsunomiya H, Sumida M et al (2016) In vitro characterization of neurite extension using induced pluripotent stem cells derived from

- lissencephaly patients with TUBA1A missense mutations. *Mol Brain* 9(1):70. <https://doi.org/10.1186/s13041-016-0246-y>
29. Yokoi S, Ishihara N, Miya F, Tsutsumi M, Yanagihara I, Fujita N, Yamamoto H, Kato M et al (2015) TUBA1A mutation can cause a hydranencephaly-like severe form of cortical dysgenesis. *Sci Rep* 5: 15165. <https://doi.org/10.1038/srep15165>
 30. Fallet-Bianco C, Laquerrière A, Poirier K, Razavi F, Guimiot F, Dias P, Loeuillet L, Lascelles K et al (2014) Mutations in tubulin genes are frequent causes of various foetal malformations of cortical development including microlissencephaly. *Acta Neuropathol Commun* 2:69. <https://doi.org/10.1186/2051-5960-2-69>
 31. Shimojima K, Narita A, Maegaki Y, Saito A, Furukawa T, Yamamoto T (2014) Whole-exome sequencing identifies a de novo TUBA1A mutation in a patient with sporadic malformations of cortical development: a case report. *BMC Res Notes* 7:465. <https://doi.org/10.1186/1756-0500-7-465>
 32. Jansen AC, Oostra A, Desprechins B, De Vlaeminck Y, Verhelst H, Régal L, Verloo P, Bockaert N et al (2011) TUBA1A mutations: from isolated lissencephaly to familial polymicrogyria. *Neurology* 76(11):988–992. <https://doi.org/10.1212/WNL.0b013e31821043f5>
 33. Okumura A, Hayashi M, Tsurui H, Yamakawa Y, Abe S, Kudo T, Suzuki R, Shimizu T et al (2013) Lissencephaly with marked ventricular dilation, agenesis of corpus callosum, and cerebellar hypoplasia caused by TUBA1A mutation. *Brain and Development* 35(3):274–279. <https://doi.org/10.1016/j.braindev.2012.05.006>
 34. Tischfield MA, Cederquist GY, Gupta ML, Engle EC (2011) Phenotypic spectrum of the tubulin-related disorders and functional implications of disease-causing mutations. *Curr Opin Genet Dev* 21(3):286–294. <https://doi.org/10.1016/j.gde.2011.01.003>
 35. Bittermann E, Abdelhamed Z, Liegel RP, Menke C, Timms A, Beier DR, Stottmann RW (2019) Differential requirements of tubulin genes in mammalian forebrain development. *PLoS Genet* 15(8): e1008243. <https://doi.org/10.1371/journal.pgen.1008243>
 36. Veldman MB, Bembem MA, Goldman D (2010) Tuba1a gene expression is regulated by KLF6/7 and is necessary for CNS development and regeneration in zebrafish. *Mol Cell Neurosci* 43(4): 370–383. <https://doi.org/10.1016/j.mcn.2010.01.004>
 37. Aiken J, Buscaglia G, Bates EA, Moore JK (2017) The α -tubulin gene TUBA1A in brain development: a key ingredient in the neuronal isotype blend. *J Dev Biol* 5(3). <https://doi.org/10.3390/jdb5030008>
 38. Gartz HM, Aiken J, Sietsema DV, Sept D, Bates EA, Niswander L, Moore JK (2016) Novel α -tubulin mutation disrupts neural development and tubulin proteostasis. *Dev Biol* 409(2):406–419. <https://doi.org/10.1016/j.ydbio.2015.11.022>
 39. Shimojima K, Okumura A, Hayashi M, Kondo T, Inoue H, Yamamoto T (2015) CHCHD2 is down-regulated in neuronal cells differentiated from iPS cells derived from patients with lissencephaly. *Genomics*. 106(4):196–203. <https://doi.org/10.1016/j.ygeno.2015.07.001>
 40. Sui H, Downing KH (2010) Structural basis of interprotofilament interaction and lateral deformation of microtubules. *Structure*. 18(8):1022–1031. <https://doi.org/10.1016/j.str.2010.05.010>

Publisher's Note Springer Nature remains neutral with regard to jurisdictional claims in published maps and institutional affiliations.